

THERMAL PROPERTIES, STRUCTURE AND MORPHOLOGY OF GRAPHENE REINFORCED POLYETHYLENE TEREPHTHALATE/POLYPROPYLENE NANOCOMPOSITES

(Sifat Termal, Struktur dan Morfologi Graphene Bertetulang Polietilena Tereftalat /Polipropilena)

I. M. Inuwa, A. Hassan*, S. A. Shamsudin

*Department of Polymer Engineering,
Faculty of Chemical and Natural Resources Engineering,
Universiti Teknologi Malaysia, UTM 81310, Skudai, Johor Darul Takzim, Malaysia*

*Corresponding author: azmanh@cheme.utm.my

Abstract

In this work the thermal properties, structure and morphology of a blend of polyethylene terephthalate (PET) and polypropylene (PP) reinforced with graphene nanoplatelets (GNP) were investigated. A blend of PET/PP (70/30 weight percent) compatibilized with styrene-ethylene-butylene-styrene grafted maleic anhydride triblock copolymer (10 phr) were fabricated by melt extrusion process in a twin screw extruder. The effective thermal conductivity of the nanocomposites increased as a function of the GNP concentration. More than 80% increase in effective thermal conductivity was observed for the 7 phr reinforced sample compared to the neat blend. This observation was attributed to the development interconnected GNP sheets which formed heat conductive bridges that are suitable for maximum heat transfer. However, in the case of thermal stability which is a function of dispersibility of GNP in polymer matrix, the maximum increase was observed at 3 phr GNP loading which could be attributed to the uniform dispersion of GNPs in the matrix... It is explained that the GNP nanofillers migrated to the surface of matrix forming an effective oxygen barrier due to char formation. Morphological studies revealed uniform dispersion graphene in the polymer matrix at 3 phr GNP loading along with isolated instances of exfoliation of the graphene layers.

Keywords: Thermal conductivity, thermal stability, polyethylene terephthalate, polypropylene, graphene nanoplatelets

Abstrak

Dalam kajian ini, sifat haba, struktur dan morfologi adunan polietilena tereftalat (PET) dan polipropilena (PP) diperkukuhkan dengan nanoplatlet grafit berkelupasan (GNP) telah dikaji. Adunan PET / PP (70/30 peratus berat) diserasikan dengan kopolimer triblok maleat anhidrida terangkuk stirena-etilena-butilena-stirena (10 phr) telah dipalsukan oleh proses penyemperitan mencairkan dalam ekstruder skru berkembar. Keberaliran haba berkesan daripada nanokomposit meningkat sebagai fungsi kepekatan GNP. Peningkatan lebih daripada 80% dalam kekonduksian terma berkesan diperhatikan untuk sampel diperkukuhkan 7 phr berbanding dengan gabungan kemas. Pemerhatian ini disebabkan oleh pembangunan saling kunci GNP yang membentuk jambatan haba konduktif yang sesuai untuk pemindahan haba maksimum. Walau bagaimanapun, dalam kes kestabilan terma yang merupakan fungsi penyerakan GNP dalam matriks polimer, peningkatan maksimum diperhatikan pada kandungan 3 phr GNP yang boleh dikaitkan dengan penyebaran seragam GNPs dalam matriks. Ia menjelaskan bahawa yang pengisi nano GNP berhijrah ke permukaan matriks membentuk halangan oksigen yang berkesan kerana pembentukan char. Kajian morfologi mendedahkan penyebaran seragam graphene dalam matriks polimer pada kandungan 3 phr GNP bersama-sama dengan kes terencil pengelupasan lapisan graphene.

Kata kunci: kekonduksian terma, kestabilan terma, polietilena tereftalat, polipropilena, nanoplatlet graphene

Introduction

Engineering thermoplastics such as polyamides, or polycarbonates, possess superior mechanical and thermal properties, and hence are finding widespread use as structural materials in such areas as the automobile, aircraft or electrical/electronic industries. Consequently, growing demand has led to a hike in prizes of these thermoplastics. It

is predicted that the global revenue for engineering thermoplastics will hit 77 billion dollars by the year 2017 [1]. However, the increasing cost of engineering thermoplastics has motivated researchers both in academia and industry into focusing attention towards finding cheaper alternatives. Commodity thermoplastics such as polyethylene terephthalate (PET) or polypropylene (PP) are relatively inexpensive but have lower performance mechanical and thermal properties when compared to engineering thermoplastics. PET is a semicrystalline commodity thermoplastic with good mechanical properties, low melt viscosity, and spinnability. PET has been used in several fields such as food packaging, film technology, automotive, electrical, beverages containers and textile fibers [2]. Although PET is widely used in the fibers and packaging industries, its use in areas where high thermal stability and thermal conductivity are required is severely limited due its poor thermal stability and conductivity. Such areas include but not limited to heat dissipation in electrical/electronic components. Blending PET and PP would offer an opportunity to combine the excellent properties of the two polymers due to synergistic effect and to overcome their individual shortcomings. Since PET and PP are thermodynamically incompatible due to differences in chemical structure and polarity, the use of suitable compatibilizers is then necessary in order to produce a material with desired properties. Elastomeric compatibilizers such as styrene-ethylene-butylene-styrene-g-maleic anhydride (SEBS-g-MAH) has led to remarkable enhancement of impact properties of PET/PP blends but has also deteriorated other properties such as stiffness and strength [3]. Thermally conductive polymer nanocomposites, offer new possibilities for replacing metal parts in several applications including power electronics, electric motors, generators and heat exchangers due to their light weight, low cost and ease of production.

Recently there has been increasing interest in the use of exfoliated graphite nanoplatelets (GNP) as a multifunctional reinforcement phase in polymer nanocomposites. These graphitic nanoplatelets, derived from graphite, combine the low-cost and layered structures of nanoclays with a unique plethora of properties usually exhibited by carbon nanotubes including electrical conductivity, superior mechanical, physical, thermal and flame retardants properties. Presently, research activities into the properties and structure of graphene has moved from curiosity-oriented to application-oriented [4,5]. Graphene is a monolayer carbon nano particle that consists of sp^2 hybridized carbon atoms arranged in hexagonal planar structures. Properties that have endeared this unique material to diverse applications are its exceptional mechanical strength (Young's modulus of 1 TPa, tensile strength of 20 GPa) [6, 7], excellent electrical (5000 S/m) [8] thermal conductivities and stability (~ 3000 W/m.K) [9]. Therefore, it is logical to assume that incorporating graphene and its derivatives (e.g. GNP) into polymeric matrices will impart significantly on thermal stability and thermal conductivity of the host polymers. Consequently, several studies have been reported on the development of multifunctional polymer nanocomposites (PNC) [10-15] using GNP as the reinforcement phase.

Several studies have been conducted to assess the thermal conductivity of graphene reinforced polymer nanocomposites [16-19]. Min et al [20] observed 157% increases in thermal conductivity of graphite nanoplatelets/epoxy composites over that of pure epoxy . Teng et al [17] studied the effect of non-covalent functionalized graphene on epoxy composites and observed remarkable improvement in thermal conductivity much higher than epoxy reinforced with multi wall carbon nanotubes. Steady state thermal analysis is a method of measurement of thermal conductivity of polymer composites and nanocomposites. This method is useful for specimens having thermal resistance in the range of 10 to 400×10^{-4} m².K/W. which can be obtained from materials of thermal conductivity in the approximate range from 0.1 to 30 W/(m.K) [21]. Although GNPs have been used to improve thermal stability and thermal conductivity in polymer nanocomposites with promising results, its use to improve the thermal conductivity of widely used commodity thermoplastics such as PET and PP or their blends is still lacking.

In this study, thermal conductivity, thermal stability, thermal behavior, morphological features and structure of GNP reinforced polyethylene terephthalate/polypropylene blends were investigated as a function of concentration of GNPs. SEBS-g-MAH is expected to serve a dual function, to compatibilize PET/PP blends and to aid the dispersion of GNPs in the polymer matrix. Conventional melt extrusion process is used to prepare PET/ PP/GNP nanocomposites because it is more economical, compatible with industrial processes (extrusion and compression molding) and free of environmentally harmful or dangerous solvents as might be encountered with other methods. To the best of our knowledge no similar report for same polymer system is published in the open literature.

Materials and Methods

Materials

Exfoliated graphite nanoplatelets, GNP-M-5 grade (99.5% carbon) of average diameter 5 μm and average thickness of less than 10 nm were purchased as dry powder from XG Sciences, Inc. (East Lansing, MI, USA) and used as received. Polyethylene terephthalate (grade M100) was obtained from Espet Extrusion Sdn Bhd (Malaysia) with intrinsic viscosity of 0.82 g/dl. PP, a copolymer grade (SM240) with density of 0.96 g/cm³ and melt flow index of 35 g/10 min (230°C and 2.16 kg load) was supplied by Titan chemicals (Malaysia). Styrene-ethylene-butylene-styrene triblock copolymer grafted with 1.84 wt % of maleic anhydride (SEBS-g-MAH) was supplied by Shell Chemical Company under the trade name of Kraton FG 1901X with ratio of styrene to ethylene/butylene in the triblock copolymer is 30/70 wt %. Melt flow index (MFI) = 20g/10 min (270°C, 5kg), molecular weight of styrene block is 7000g/mol. and ethylene/butylene block is 37500g/mol.

Blends and Nanocomposites fabrication

PET was pre-dried in vacuum oven at 120 °C for 48 hours, PP was dried at 80 °C for 24 hours and SEBS-g-MAH was dried for 8 hours at 60 °C. PET, PP, SEBS-g-MAH and GNP with various ratios were melt blended using a counter-rotating twin screw extruder (Brabender Plasticoder, P 2000). All materials were compounded in a single step with various amounts of GNPs according to sample formulation Table shown in Table 1. The temperature setting from the hopper to the die were 265/275/280/285 °C and the screw speed was 60 rpm. The composites were pelletized and then dried at 100 °C for 12 hours before pressing into sheets of 3mm thickness using a hydraulic press set at a temperature of 250°C for both lower and upper plates and 100 psi pressure.

Table 1. Sample Formulations (70 wt% PET, 30 wt % PP, and 10 wt% SEBS-g-MAH) with GNP variation.

| Sample name | GNP (phr) |
|-------------|-----------|
| GNP0 | 0 |
| GNP1 | 1 |
| GNP2 | 2 |
| GNP3 | 3 |
| GNP4 | 4 |
| GNP5 | 5 |
| GNP6 | 6 |
| GNP7 | 7 |

Nanocomposites characterization

Cussons thermal conductivity analyser was used to measure the thermal conductivity of various materials, which include polymers, glasses, ceramics, rubbers composites, few metals and other materials with medium to low thermal conductivity by steady state method. In the present work, this instrument is used to measure the room temperature effective thermal conductivity of the composites specimens. This test is conducted in accordance with ASTM E1530 standards. The material was held under uniform compressive load between two polished surfaces, each controlled at a different temperature. The lower surface is part of a calibrated heat flow transducer. The heat flows from the upper surface through the sample to the lower surface establishing an axial temperature gradient in the stack. After reaching thermal equilibrium (steady state), the temperature difference across the sample was measured along with the output from the heat flow transducer. The temperature difference and the sample thickness were then used to calculate the effective thermal conductivity using equation 1. The temperature drop through the

sample was measured with temperature sensors in the highly conductive metal surface layers on either side of the sample. By definition thermal conductivity is the exchange of energy between adjacent molecules and electrons in a conducting medium, it is material property that describes heat flow within a body for a given temperature difference per unit area.

The thermal conductivity of nanocomposites was calculated according to equation 1.

$$k = \frac{q \cdot L}{T_1 - T_2} \quad (1)$$

k = thermal conductivity (W/mK),

q = heat flow (W/m²)

L = specimen thickness (m),

T₁ = temperature of one surface of the specimen (°C),

T₂ = temperature of the other surface of the specimen (°C).

Thermal Stability

In order to examine the thermal degradation behavior of samples, thermogravimetric analysis (TGA) was performed on Perkin Elmer TGA 7 instrument at a rate of 10°C/min under nitrogen atmosphere in the temperature range 30 – 600°C.

Differential Scanning Calorimetry

The melting and crystallization behavior of PET/PP and PET/PP/GNP composites were characterized through differential scanning calorimetry (DSC) (Perkin Elmer DSC-6), using 5-10 mg samples sealed in aluminum pans. The temperature was raised from 30 to 300 °C at a heating rate of 10°C/min, and after a period of 1 min, it was swept back at the rate of 10°C/min. The fusion enthalpies, ΔH_f(PET) and ΔH_f(PP) were measured and the degree of crystallinity, X_c(PET) and X_c(PP) were calculated using the following equations 2 and 3 :

$$\%X_c(PET) = \frac{\Delta H_f(PET)}{\Delta H_f^0(PET)} \times \frac{1}{W(PET)} \times 100 \quad (2)$$

$$\%X_c(PP) = \frac{\Delta H_f(PP)}{\Delta H_f^0(PP)} \times \frac{1}{W(PP)} \times 100 \quad (3)$$

ΔH_f⁰(PET) = 140 J/g and ΔH_f⁰(PP) = 209J/g [22]. Where w_{PET} and w_{PP} are the weight fractions of PET and PP, respectively

Morphological characterization

Dispersion of the graphite nanoplatelets was observed using field emission scanning electron microscopy (FESEM) and transition electron microscopy (TEM). FESEM micrographs of fractured surfaces of the unreinforced blend and nanocomposites were obtained using a Hitachi S-4800. The blend control and the nanocomposites were gold coated using a Balzers Union MED 010 coater. For TEM analysis, a thin section (thickness of 70 nm) was used for transmission imaging. Samples were microtomed using Reichert Jung Ultracut E microtome. Transmission micrographs were collected using a JEOL JEM-2100 microscope, with an operating voltage of 200 kV.

X-ray diffraction analysis

X-ray diffraction patterns were collected using X'Pert, X-ray diffractometer (Siemens XRD D5000) and Ni-filtered Cu Kα radiation at an angular incidence of 0° to 70°(2θ angle range). XRD scans of the GNP powder along with the composites samples were collected at 40 kV and 50 mA with an exposure time of 120s. Diffraction patterns were obtained using equation 4 to evaluate the dispersion of GNPs in the matrix.

$$n\lambda = 2\theta \sin \theta_p \quad (4)$$

where θ_p = diffraction angle of the primary diffraction peak and λ = X-ray wave length, n = 1.

Results and Discussion

Thermal Conductivity

The effect of GNP loading on effective thermal conductivity of PET/PP/GNP nanocomposites is shown in Fig. 1 below. The effective thermal conductivity of PET/PP/GNP nanocomposites was increased with increase in GNP concentration. However, sharp rise in the effective thermal conductivity can be seen at 3 phr GNP loading which corresponds to the establishment thermal percolation threshold. Chu *et al* [23] in their recent work, “Thermal conductivity of composites with hybrid carbon nanotubes and graphene nanoplatelets”, have elaborated on the concept of thermal percolation threshold of graphite nanoplatelets.

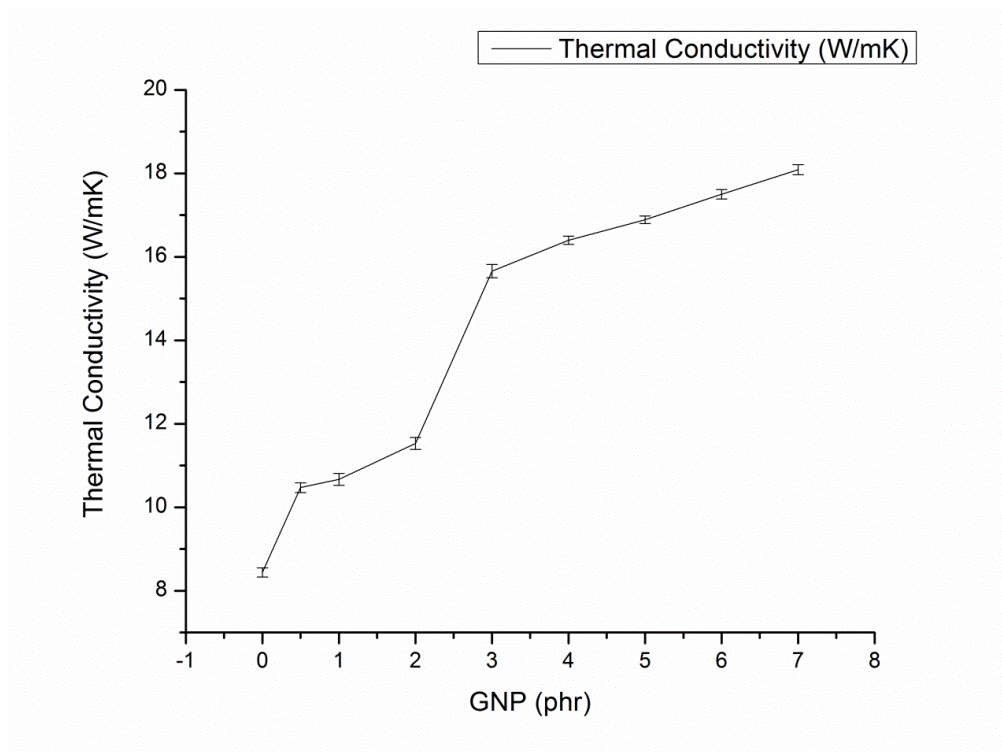


Figure 1. Effect of GNP loading on effective thermal conductivity of PET/PP/GNP nanocomposites

The thermal conductivity of 7 phr reinforced PET/PP/GNP nanocomposites was 18.709 W/mK, more than two times improvement compared that of the neat PET/PP blends. It can be seen that the relative increase in the effective thermal conductivity is higher with increase in GNP loading beyond the established percolation threshold at 3 phr. This observation is presumed to correspond to the development of effective interconnected GNP network that is most suitable for heat transfer. Prior to this filler concentration, the GNPs are thought to be randomly distributed in the polymer matrix standing isolated without contact to each other as depicted in the illustrated scheme in Fig. 2 which led to low efficiency for thermal conductivity [21]. This resulted in lower improvement in the values of the effective thermal conductivity. At higher concentration the GNP platelets are aligned and overlapped with each other leading to development of effective interconnected network that sharply enhanced thermal conductivity at 3 phr GNP loading.

Recently, it was found that fillers with high aspect ratio, such as whiskers and platelets, can form more continuous thermally conductive network in the polymer matrix and thus more effective in enhancing thermal transfer [19].

This factor combined with the high intrinsic thermal conductivity of GNPs offered reasonable explanations for the larger increments of thermal conductivity of PET/PP/GNP with increasing filler content. Due to Van der Waals' attraction a homogenous GNP network could be achieved under relatively high filler content. This evidence can be corroborated by the TEM micrographs of the PET/PP/GNP nanocomposites (3 phr filler level). The formation GNP interconnected network would also ensure the decrease in scattering of phonon transfer and promote the diffusion of phonons in the overall nanocomposites. Similar observation has been made in the polymeric systems filled with hybrid GNP/carbon nanotubes [24].

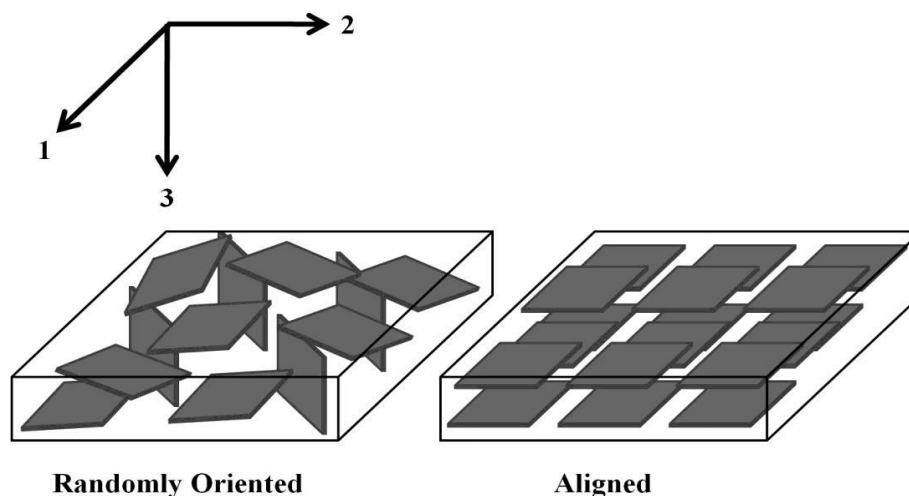


Figure 2. Distribution of GNPs in PET/PP; random orientation (low GNP concentration) and aligned orientation (higher GNP concentration at 3phr and above)

FESEM Analysis

Studies of the surface morphology and compositions of polymer nanocomposites by FESEM have been used extensively to characterize the dispersion of nanofillers in polymeric matrices [25,26]. Fig.3 is a typical FESEM of PET/PP blends and PET/PP/GNP nanocomposites. Fig. 3a shows the FESEM micrograph of unreinforced PET/PP blend. It is interesting to note that addition of SEBS-g-MAH has compatibilized the immiscible PET/PP blend (shown by arrow) by reducing the particle size of the dispersed PP phase and eliminating the voids. This resulted in the improved adhesion of the different phases and reduced interfacial tension. Similar finding was reported by Heino et al [27]. FESEM image of the impact fractured surface of PET/PP/GNP nanocomposites taken in the transverse direction is depicted in Fig.3b. The GNPs appear to be embedded and uniformly dispersed in the nanocomposites with the edges of the graphene sheets projecting out of the fractured surface. The uniform dispersion of GNPs in the polymer matrix is responsible for the observed increase in the properties. This observation is consistent with that of Ramanathan et al. [28]. Fig.3c shows the interaction of the GNP particles with the SEBS-g-MAH particles as shown by arrow. The compatibilizer can be seen attached to the surface of GNP sheets. This indicates that the compatibilizer functions by aiding the dispersion of GNPs in the polymer matrix through encapsulation of GNPs by the rubber particles in addition to improving the adhesion between PET and PP particles. Similar findings were reported by Zhang and Deng [29]

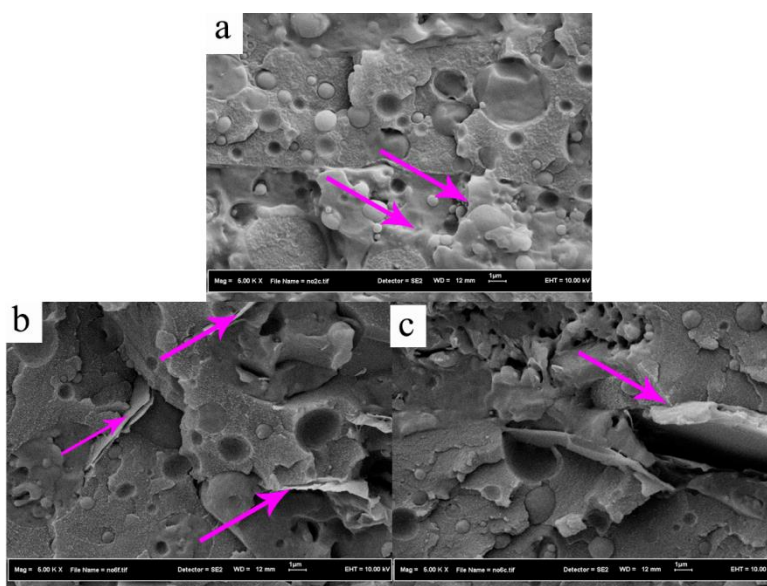


Figure 3. FESEM images of PET/PP/GNP nanocomposites at 3 phr showing a) pure PET formation of b) PET/PP blend c) uniform dispersion of GNP d) attachment of GNP particles on the compatibilizer surface

TEM Analysis

TEM analysis is a proven and reliable technique for investigating the dispersion of nanofillers in polymer matrix. Fig.4 is the image analysis of GNP3. In Fig. 4a, the interconnected GNP sheets can be seen within the matrix with maximum of three sheets overlapping on each other. Interconnected morphology is the most suitable for improvement of transport properties such as thermal conductivity. This confirms that the number of sheets was reduced from 5 to 3 sheets originally supplied by the manufacturer which can be attributed to shear mixing in the extruder equipment. Close examination of Fig. 4b can reveal the interaction of GNP with the polymer matrix possibly SEBS-g-MAH. Folded graphene sheet off-plane, can be seen surrounded by matrix which is represented by the blurred grey background with improved adhesion by the compatibilizer elastomer particle or absorption by the PET/PP chains [32]. The shear mixing also involve wrinkling (Fig. 4c) and crumpling (Fig. 4d) of exfoliated single layers due to the thin thickness of the graphene particles. It has been reported that the presence of the wrinkled and crumpled exfoliated graphene sheets may actually lead to nanoscale surface roughness which would likely produce an enhanced mechanical interlocking and adhesion with the polymer chains [30]. It is reported that SEBS-g-MAH improved the dispersion of fillers in the polymeric matrices thereby improving the toughness and wear resistance of the matrix due to interaction with fillers [29, 31]. Overall it is evident that good dispersion of GNP sheets has been achieved with isolated instances of exfoliation.

Thermogravimetric analysis

Thermal stability of the neat blend and composites were investigated under nitrogen gas atmosphere as described section 2.3.2. The results of the measurements are shown in Fig. 5a, and 5b respectively and the corresponding data is shown in Table 2. The thermal decomposition temperature of the blends and composites show a single step decomposition process indicating effective compatibilization of the blends. The results also show the effect of GNPs on the thermal stability of the neat PET/PP blends. From Table 2, the T_{10} and T_{50} as well as maximum decomposition temperatures T_{max} are characteristically high for all the composites compared with the neat blend. In particular, the 3 phr GNP concentration yielded highest thermal stability.

The enhanced thermal stability of the composites was attributed to the high aspect ratio of GNPs which serve as a barrier and prevented the emission of gaseous molecules during thermal degradation. The dramatic improvement at

3.0 phr is attributed to the homogenous dispersion of the GNPs in the matrix at this filler level. Homogeneously dispersed GNP disrupted the oxygen supply by forming charred layers on the surfaces of the composites thereby enhancing thermal stability [32]. However the weight residue shows that highest amount of ash was obtained with the 5.0 phr GNP loading. This logically means that as the quantity of the GNP increased the residue was also increased due to very high thermal stability of the graphene platelets. These observations are consistent with those made by Tantis et al. [33].

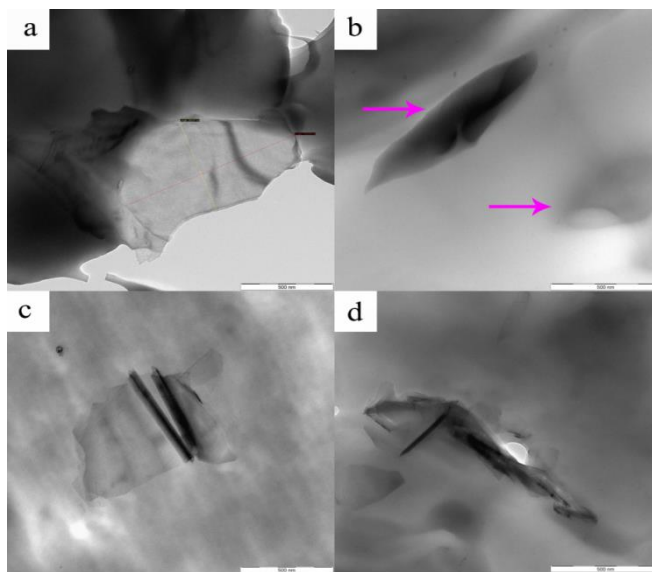


Figure 4. a) Interconnected GNP sheets at 3 phr loading, b) adhesion of GNP to polymer matrix promoted by SEBS-g-MAH, c) wrinkled GNP sheets and d) crumpled GNP sheets.

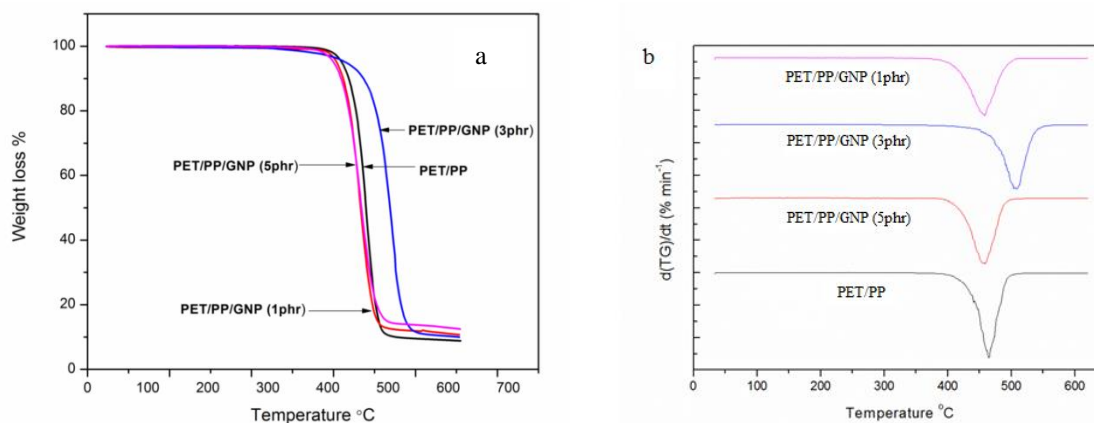


Figure 5. a) TGA and b) DTG curves of neat PET/PP and PET/PP/GNP nanocomposites

Table 2. TGA and DTG data

| Sample | Degradation Temp (°C) | | DTG Peak Temp | Residual Weight (%) at 600°C |
|-------------|-----------------------|-----------------|------------------|------------------------------|
| | T ₁₀ | T ₅₀ | T _{max} | |
| Neat Blend | 424°C | 454°C | 466°C | 8.774 |
| GNP 1.0phr | 426°C | 457°C | 457°C | 10.068 |
| GNP 3.0 phr | 458 °C | 502 °C | 505°C | 11.808 |
| GNP 5.0 phr | 421°C | 456°C | 455°C | 12.867 |

Differential Scanning Calorimetry

Fig. 6a and b show the heating and cooling scans of DSC traces for blends and nanocomposites. The corresponding thermal data is provided in Table 3. From the Table it is clear that the T_c values of all nanocomposites are higher than those of the unreinforced PET/PP blend and increase with increasing GNP content. This phenomenon can be explained by the heterogeneous nucleation effect of the GNPs on the chain segments, which leads to the crystallization of PET at higher temperatures. Similar explanation can be made for the T_{c,pp}. This is consistent with previous studies [34].

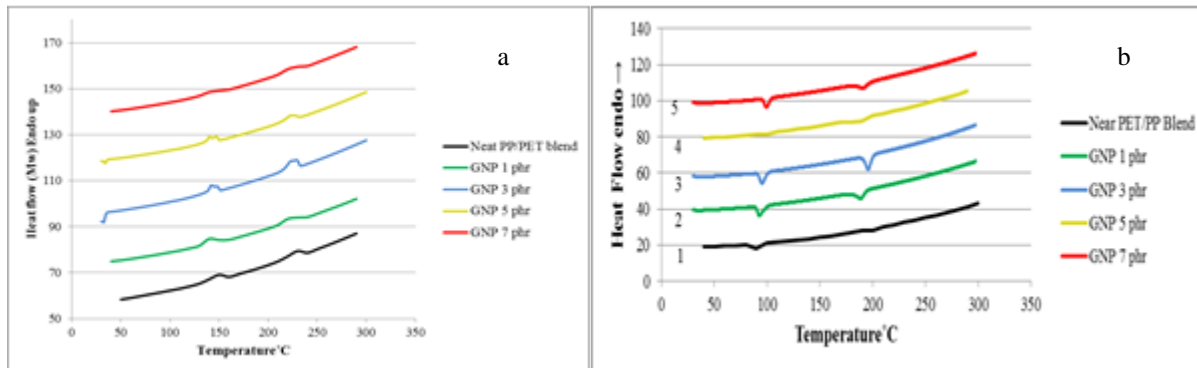


Figure 6. DSC plots a) Heating scans and b) cooling scans of PET/PP, PET/PP/GNP nanocomposites

However, the crystallinity of PET and PP in PET/PP/GNP nanocomposites decreased with the addition of GNP. It can be thought that the presence of GNP has restricted the mobility of PET and PP chains during the crystallization process. The high surface area of the GNP sheets enables them to act as vast heterogeneous nucleation points which increased crystallization rates. Subsequently less crystalline regions are formed due to shorter time available. Additionally, due to the nanosized dimension of GNP particles; they can present in both PET and PP phases resulting in the increased T_c for both PET and PP. The T_m of both PET and PP however, remain essentially unaffected. Karevan and Kalaitzidou [35] observed that the decrease in the degree of crystallinity of PA12 with GNP content may be due to the decrease in the free volume and constrains of the polymer chains imposed by the rigid GNP that do not allow them to rearrange and form crystals.

Table 3. DSC data of PET, PET/PP and PET/PP/GNP nanocomposites

| Designation | Crystallization Temperature °C | | Melting Temperature °C | | Crystallinity (%) | |
|-------------|--------------------------------|-------|------------------------|-------|-------------------|------|
| | PET | PP | PET | PP | PET | PP |
| GNP0 | 178.1 | 89.3 | 230.1 | 150.4 | 24.1 | 19.8 |
| GNP1 | 189.7 | 93.3 | 230.0 | 140.6 | 21.6 | 17.6 |
| GNP3 | 196.3 | 97.4 | 229.8 | 148.4 | 20.2 | 15.3 |
| GNP5 | 186.5 | 99.5 | 228.7 | 148.3 | 19.5 | 13.4 |
| GNP7 | 190.2 | 100.0 | 230.1 | 150.5 | 19.0 | 12.1 |

X-Ray Diffraction

The XRD patterns of the pristine GNP, neat PET/PP blend and PET/PP/GNP composites are shown in Fig. 7. The characteristic peaks of diffraction pattern for the graphene nanoplatelets shows the graphene-2H characteristic peaks at 26.6° ($d=3.35 \text{ \AA}$) and 54.7° ($d=1.68 \text{ \AA}$) 2θ . The absence of the characteristic graphene peaks in the nanocomposites along with the observations by TEM and FESEM suggest a uniform dispersion of GNP sheets in the matrix. It may be concluded that GNPs in the composites may not have been substantially exfoliated but homogeneously distributed in the matrix thereby improving the properties. Bandla et al. [36] have reported similar observations.

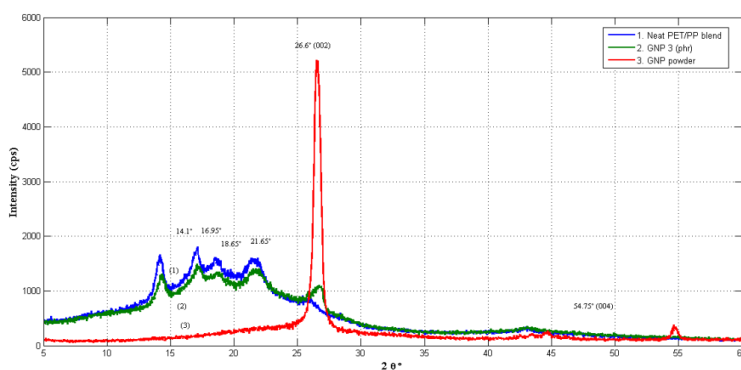


Figure 7. X-ray diffraction features of the neat PET/PP blends GNP powder and PET/PP/GNP nanocomposites

Conclusion

Nanocomposites based on blends of PET/PP compatibilized with SEBS-g-MAH and GNPs have been successfully prepared by melt extrusion technique. Thermal conductivity, thermal behavior, morphological features and structure of the resulting nanocomposites were investigated. Thermal conductivity exhibited linear relationship with increased GNP loading with percolation established at 3 phr loading. This was attributed to the development of effective heat conduction bridges of interconnected GNPs that increased the efficiency for thermal conductivity. Morphological features show uniform dispersion and the development of interconnected GNP sheets at 3 phr loading with isolated instances of exfoliated GNP sheets. Addition of GNPs also led to decrease in the degree of crystallinity of PET/PP/GNP nanocomposites and the melting temperature remained almost the same. This study has showed the potential of using GNPs to develop a thermally conductive polymer nanocomposites based on

blends of PET/PP blends for applications in electrical/electronics industry where heat dissipation in electrical components are essential.

Acknowledgement

The authors would like to thanks Ministry of Higher Education of Malaysia (MOHE) and Universiti Teknologi Malaysia (UTM) for Research Universiti Grant vote number 02H26 and sub code Q.J130000.7113.02H26.

References

1. Emory, K. (2013). The eco-friendly car is driving engineering plastics market to \$76 billion by 2017. Retrieved 12 January, 2014, from <http://www.tgdaily.com/general-sciences-features/78573-the-eco-friendly-car-is-driving-engineering-plastics-market-to-76-bi#VRkDTSm6J5LpjbcK.99>
2. Bartolome, L., Imran, M. and Cho, B.G. (2012). Recent Developments in the Chemical Recycling of PET in Material Recycling – Trends and Perspectives. ed. Achilias, D. S. 65-84.
3. Abdul Razak, N. C., Inuwa, I. M., Hassan, A. & Samsudin, S. A. (2013). Effects of compatibilizers on mechanical properties of PET/PP blend. *Compos. Interfaces*, 20 (7): 507-515.
4. Liu, X.G. (2013). How will carbon material lead to a Low Carbon Society – A review of Carbon 2012. *Carbon*, 51: 438.
5. Hussain, F. H., Mehdi O., Masami Gorga, & Russell E. (2006). Review article: Polymer-matrix Nanocomposites, Processing, Manufacturing, and Application: An Overview. *J. Compos. Mater.*, 40 (17): 1511-1575.
6. Geim, A. K., & Novoselov, K. S. (2007). The rise of graphene. *Nat Mater*, 6 (3): 183-191.
7. Lee, C. W., Xiaoding K., Jeffrey W. & Hone, J. (2008). Measurement of the Elastic Properties and Intrinsic Strength of Monolayer Graphene. *Science*, 321 (5887): 385-388.
8. Zhang, Y. A., Dervishi, S. F., Xu, E., Li, Y., Casciano, Z. & Biris, D. A. S. (2010). Cytotoxicity effects of graphene and single-wall carbon nanotubes in neural pheochromocytoma-derived PC12 cells. *ACS Nano*, 4: 3181.
9. Balandin, A. A., Ghosh, S.B., Wenzhong, C., Teweldebrhan, I., Miao, D., Lau, F. & Ning, C. (2008). Superior Thermal Conductivity of Single-Layer Graphene. *Nano Lett.*, 8 (3): 902-907.
10. Kuila, T. B., Saswata, K., Partha, K., Nam, H. R., Kyong, Y. L., & Joong, H. (2011). Characterization and properties of in situ emulsion polymerized poly(methyl methacrylate)/graphene nanocomposites. *Composites Part A*, 42 (11): 1856-1861.
11. Kuila, T. B., Saswata, K., Partha, K., Nam, H. R., Kyong, Y. L., & Joong, H. (2012). Effect of functionalized graphene on the physical properties of linear low density polyethylene nanocomposites. *Polym. Test.*, 31 (1): 31-38.
12. Zhao, X. Z., Qinghua, C. & Dajun, L. (2010). Enhanced Mechanical Properties of Graphene-Based Poly(vinyl alcohol) Composites. *Macromolecules*, 43 (5): 2357-2363.
13. Rafiee, M. A., Rafiee, J., Wang, Z., Song, H., Yu, Z. Z. & Koratkar, N. (2009). Enhanced mechanical properties of nanocomposites at low graphene content. *ACS Nano*, 3: 3884.
14. Haafiz, M. K., Hassan, A., Zakaria, Z. & Inuwa, I. M. (2014). Isolation and characterization of cellulose nanowhiskers from oil palm biomass microcrystalline cellulose. *Carbohydr. Polym.*, 103: 119-125.
15. Bandla, S. & Hanan, J. C. Manufacturing tough amorphous thermoplastic-graphene nanocomposites. in Nanotechnology 2012: Advanced Materials, CNTs, Particles, Films and Composites - 2012 NSTI Nanotechnology Conference and Expo, NSTI-Nanotech 2012. 2012. Santa Clara, CA.
16. Prusty, G. S. & Sarat K. (2013). Dispersion of expanded graphite as nanoplatelets in a copolymer matrix and its effect on thermal stability, electrical conductivity and permeability. *Carbon*, 51: 436.
17. Teng, C. C. M., Chen-Chi, M. L., Chu-Hua, Y., Shin-Yi, L., Shie-Heng, H., Min-Chien, Y., Ming-Yu, C., Kuo-Chan, L. & Tzong, M. (2011). Thermal conductivity and structure of non-covalent functionalized graphene/epoxy composites. *Carbon*, 49 (15): 5107-5116.
18. Jiang, X. D. & Lawrence, T. (2012). Exploring the potential of exfoliated graphene nanoplatelets as the conductive filler in polymeric nanocomposites for bipolar plates. *J. Power Sources*, 218: 297-306.
19. Yu, S., Jeong, S.G., Chung, O. & Kim, S. (2014). Bio-based PCM/carbon nanomaterials composites with enhanced thermal conductivity. *Sol. Energy Mater. Sol. Cells*, 120, Part B: 549-554.

20. Min, C. Y., Demei, C., Jingyu, W. & Lihua, G.F. (2013). A graphite nanoplatelet/epoxy composite with high dielectric constant and high thermal conductivity. *Carbon*, 55: 116-125.
21. Han, Z. & Alberto, F. (2011). Thermal conductivity of carbon nanotubes and their polymer nanocomposites: A review. *Prog. Polym. Sci.*, 36 (7): 914-944.
22. Li, W., Schlarb, A. K. & Evstatiev, M. (2009). Study of PET/PP/TiO₂ microfibrillar-structured composites, part 1: Preparation, morphology, and Dynamic mechanical analysis of fibrillized blends. *J. Appl. Polym. Sci.*, 113 (3): 1471-1479.
23. Chu, K., Li, W.S., Jia, C. C. & Tang, F. L. (2012). Thermal conductivity of composites with hybrid carbon nanotubes and graphene nanoplatelets. *Appl. Phys. Lett.*, 101 (21).
24. Huang, X., Zhi, C. & Jiang, P. (2012). Toward effective synergetic effects from graphene nanoplatelets and carbon nanotubes on thermal conductivity of ultrahigh volume fraction nanocarbon epoxy composites. *J. Phys. Chem. C*, 116 (44): 23812-23820.
25. Verdejo, R., Bernal, M., Mar, R., Laura, J., Machado, L. & Miguel A. (2011). Graphene filled polymer nanocomposites. *J. Mater. Chem.*, 21 (10): 3301-3310.
26. Wakabayashi, K., Brunner, P. J., Masuda, J., H., Sheldon A., & Torkelson, J. M. (2010). Polypropylene-graphite nanocomposites made by solid-state shear pulverization: Effects of significantly exfoliated, unmodified graphite content on physical, mechanical and electrical properties. *Polymer*, 51 (23): 5525-5531.
27. Heino, M., Kirjava, J., Hietaoja, P. & Seppala, J. (1997). Compatibilization of polyethylene terephthalate/polypropylene blends with styrene-ethylene/butylene-styrene (SEBS) block copolymers. *J. Appl. Polym. Sci.*, 65 (2): 241-249.
28. Ramanathan T., Stankovich S., Dikin D. A., Liu, H. Shen, H. Nguyen S. T., Brinson, L. C. (2007). Graphitic nanofillers in PMMA nanocomposites—An investigation of particle size and dispersion and their influence on nanocomposite properties. *J. Polym. Sci., Part B: Polym. Phys.*, 45 (15): 2097-2112.
29. Zhang, J. G. & Deng J. (2011). Effect Of SEBS- g -MA on wear friction of PA6-CNT composite. *Polym-Plast Technol*, 50: 1533–1536.
30. Ramanathan, T. Abdala, A. A. Stankovich, S. Dikin, D. A. Herrera-Alonso, M. Piner, R. D. Adamson, D. H. Schniepp, H. C. Chen, X. Ruoff, R. S. Nguyen, S. T. Aksay, I. A. nPrud'homme, R. K. & Brinson, L. C. (2008). Functionalized graphene sheets for polymer nanocomposites. *Nat. Nanotechnol.*, 3 (6): 327-331.
31. Lim, S. R. & Chow, W. S. (2012). Impact, thermal, and morphological properties of functionalized rubber toughened-poly(ethylene terephthalate) nanocomposites. *J. Appl. Polym. Sci.*, 123 (5): 3173-3181.
32. Li, M., & Jeong, Y. G. (2011). Poly(ethylene terephthalate)/exfoliated graphite nanocomposites with improved thermal stability, mechanical and electrical properties. *Composites Part A*, 42 (5): 560-566.
33. Tantis, I., Psarras, G. C. & Tasis. D. (2012). Functionalized graphene – poly(vinyl alcohol) nanocomposites: Physical and dielectric properties. *Express Polym Lett*, 6 (4): 283 -292.
34. Akbari, M. Zadhoush, A. Haghighat, M. (2007). PET/PP blending by using PP-g-MA synthesized by solid phase. *J. Appl. Polym. Sci.*, 104 (6): 3986-3993.
35. Karevan, M., Eshraghi, S., Gerhardt, R., Das, S., & Kalaitzidou, K. (2013). Effect of processing method on the properties of multifunctional exfoliated graphite nanoplatelets/polyamide 12 composites. *Carbon*, 64: 122-131.
36. Bandla, S. & Hanan, J. (2012). Microstructure and elastic tensile behavior of polyethylene terephthalate-exfoliated graphene nanocomposites. *J. Mater. Sci.*, 47 (2): 876-882.